Lanthanide Circularly polarised luminescence: bases and applications

Francesco Zinna and Lorenzo Di Bari*

Abstract: lanthanide (III) luminescence is very characteristic: it is characterised by narrow emission bands, large Stokes shift and long excited state lifetime. Moreover chiral lanthanide complex can emit strongly circularly polarised light in a way that is almost precluded to purely organic molecules. Thanks to the sensitivity and specificity of the Ln CPL signal, CPL-active complexes are therefore already employed as bioanalytical tools and other uses can be envisaged in other fields.

Here we aim to present a brief overview of the most recently developed CPL-active lanthanide complexes and a selected few examples of their applications. We briefly discuss the main mechanisms that can rationalise the observed outstanding CPL properties of these systems, and some practical suggestions on how to measure and report data.

Keywords: Lanthanides, chiral complexes, luminescence, circularly polarised luminescence, CPL, luminescent bioprobes, chirooptical spectroscopy, luminescence dissymmetry factor.

Introduction

Compared to *d*-metals, lanthanides (III) are endowed with peculiar spectroscopic features.[1-3] Their absorption and emission bands are narrow and the energies of their electronic transitions are largely independent of the coordination environments. They can be considered spherical emitters in solution with a long excited state life-time (up to 10 msec), so they do not require taking into account emission anisotropy.

Purely intraconfigurational *f→f* transitions are Laporte-forbidden and are associated with very small absorption bands (ε=1-10 $M^{-1}cm^{-1}$), but they can be conveniently observed in emission, once they reach an excited state by means of some energy transfer process. Usually this is made possible through a so-called *antenna effect*, which requires that the organic ligand[i] absorbs high energy radiation and passes excitation onto the Ln(III), most often through a Förster mechanism.

Lanthanide coordination chemistry is well known,[11] which allows one to rationally design ligands containing chromophoric groups: if the electronic levels of donor (ligand) and acceptor (lanthanide) match[2] and if they are in close proximity and with the correct lifetimes, the ligand-to-lanthanide energy transfer process can be quite efficient.[ii]

In fact high quantum yields have been reported especially for Eu^{3+} in the visible (red) region. At the moment, one can reasonably predict the main features of a successful complex, and justify *a posteriori* its experimental behaviour. This leads to a rational ligand design, although not always the final products meet the expectations, because of the multiple parameters involved in the process.

For these characteristics, luminescent Ln^{3+} have been employed with various purposes, such as:[12] molecular probes for biomedical imaging and sensing[9] and bioanalytical applications[13] (see below for some examples), electroluminescent devices,[14-16] in photovoltaics as spectrum downshifters,[17] in telecommunications,[18] and as dyes in security inks and labels.[3]

In addition, when the emissive complex is chiral non racemic, it may emit left and right circularly polarised light with different intensities. The phenomenon is called *circularly polarised luminescence* (hereafter *CPL*) and it is usually quantified through the l*uminescence dissymmetry factor* g_{lum}, defined as:

$$g_{\mathrm{lum}} = \frac{I_L - I_R}{1/2(I_L + I_R)} = \frac{\Delta I}{I} \qquad (1)$$

Where I_L and I_R are the left and right polarised emission intensities respectively. It follows immediately that g_{lum}= ±2 means complete polarisation of the emitted light while 0 corresponds to an unpolarised beam. While organic chiral molecules or macromolecules typically display g_{lum} values of 10^{-3}–10^{-2}, lanthanide complexes show values of 0.1–1,[19] with 1.38 being the highest value ever reported so far for a lanthanide complex[20] (and, to the best of our knowledge, one of the highest values ever measured at all).

Circularly polarised luminescence allows one to:[21]

- extract information about the chirality of the excited state (CPL is therefore complementary to circular dichroism);
- observe transitions that can not be easily observed in absorption (as it is the case with *f→f* transitions of lanthanides);
- observe only selected transitions (since one may have many chromophores but only few luminophores that respond to a certain excitation wavelength).

Lanthanide complexes are optimal candidates to be studied through CPL.

In this brief review we shall discuss some recent applications and developments of lanthanide CPL. All the following examples deal with complexes in solution: in the literature there are only rare and relatively old examples of

Dipartimento di Chimica e Chimica Industriale, Università di Pisa, via Risorgimento 35, I-56126 Pisa, Italy .

[*] *lorenzo.dibari@unipi.it*

Received: ((will be filled in by the editorial staff))
Revised: ((will be filled in by the editorial staff))
Published online: ((will be filled in by the editorial staff))

[i] There are some reports of *d-f* dimetallic complexes where the absorbing chromophore is the *d*-metal.[5-7]

[ii] This mechanism ensures large Stokes shift: 250 nm can be typical.

measurements in the solid state, although the current interest for applications of lanthanide luminescence in devices of various types should solicit more activity solid state CPL measurements.

Where to look for high g_{lum} Values

High g_{lum} values are to be sought for among electric dipole forbidden/magnetic dipole allowed transitions.

In fact, fort he transition $i \rightarrow j$ the luminescence dissymmetry factor can be written as:

$$g_{\mathrm{lum}} = 4\frac{\left|\boldsymbol{\mu}_{ij}\right| \cdot \left|\mathbf{m}_{ji}\right| \cos\theta_{\boldsymbol{\mu},\mathbf{m}}}{\left|\boldsymbol{\mu}_{ij}\right|^2 + \left|\mathbf{m}_{ji}\right|^2} \qquad (2)$$

where $\boldsymbol{\mu}_{ij}$ e $\boldsymbol{m}_{ji}$ are the electric and magnetic transition dipole vectors and $\theta_{\boldsymbol{\mu},\mathbf{m}}$ is the angle between them. In the case of an electric dipole allowed transition, the $|\mathbf{m}_{ji}|^2$ term is negligible with respect to $|\boldsymbol{\mu}_{ij}|^2$; so equation (2) becomes:

$$g_{\mathrm{lum}} = 4\frac{m_{ji}}{\mu_{ij}}\cos\theta_{\boldsymbol{\mu},\mathbf{m}} \qquad (3)$$

with the $|\boldsymbol{m}_{ji}| / |\boldsymbol{\mu}_{ij}|$ ratio being well less than 1.

Strict Laporte selection rule cannot apply in chiral molecules, because rotation-reflection (or rotoreflection) elements, like symmetry planes and inversion are excluded by chirality itself. Nonetheless, if the chromophore can be considered intrinsicallly achiral, then one can generally postulate that for some of its electronic transitions $\boldsymbol{\mu}_{ij}$ is very small so that g_{lum} may become sizeable (but in any case smaller than 2).

Richardson[22] classified lanthanide transitions in three classes (*DI*, *DII* and *DIII*) concerning the dissymmetry factor: the magnitude of the observed dissymmetry factors is expected to decrease as *DI>DII>DIII*. Richardson himself noted that the Eu^{3+} $^5D_0 \rightarrow {}^7F_1$ is the only lanthanide transition belonging to class *DI* easily accessible to CPL measurement; no wonder that the highest g_{lum} values have been measured for this transition.

Beside Eu^{3+}, CPL spectra in the visible region are commonly measured for Sm^{3+},[23,24] Tb^{3+},[23,25] and Dy^{3+}[23] complexes; in Table 1 we show the transitions generally observed in CPL measurements and their *D* class.

TABLE 1 Ln^{3+} transitions generally observed in CPL measurements with their D class[22] and their approximate wavelength.

Ion	Transition	Wavelength (nm)	Class
Sm^{3+}	$^4G_{5/2} \rightarrow {}^6H_{5/2}$	565	*DII*
	$^4G_{5/2} \rightarrow {}^6H_{7/2}$	595	*DIII*
Eu^{3+}	$^5D_0 \rightarrow {}^7F_1$	595	*DI*
Tb^{3+}	$^5D_4 \rightarrow {}^7F_5$	545	*DII*
Dy^{3+}	$^4F_{9/2} \rightarrow {}^6H_{11/2}$	670	*DIII*

CPL and total luminescence

Although the emission bands of most lanthanide complexes are very narrow, especially compared to those of organic or *d*-metal emitters, very often they display a fine structure, consisting in lines of one or a few nm width.

Taking as an example the $^5D_0 \rightarrow {}^7F_J$ transitions associated to an Eu^{3+} complex, it can be noted that the initial state is singly degenerate, while the final state is *(2J+1)*–fold degenerate in a total symmetric environment: depending on the coordination sphere this degeneracy can be removed,[26] leading to a splitting of the emission band.

The energy gap among these levels can be as small as 100–130 cm^{-1}, which translates in 5 nm or less in the yellow-orange region.

As a consequence, at room temperature, this may be only partially (if at all) resolved.

As it occurs in other spectroscopies where bands may have different signs, and very notably in electronic and vibrational CD, in CPL there may be an apparent resolution enhancement when nearby transitions have opposite rotational strengths.

This is notably the case of the CPL spectrum shown in Figure 1, concerning the $^5D_4 \rightarrow {}^7F_5$ transition of a Tb^{3+} chiral complex.[27]

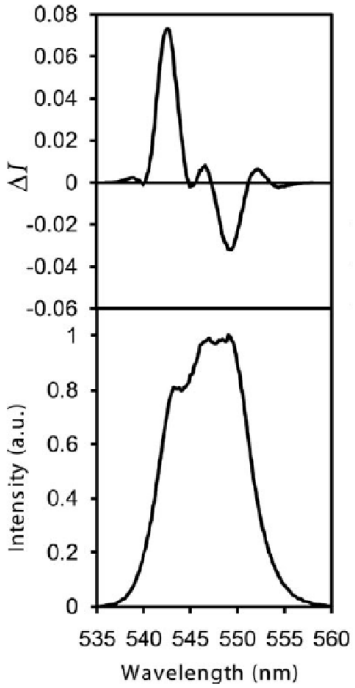

FIGURE 1: CPL and total emission of a Tb^{3+} complex for $^5D_4 \rightarrow {}^7F_5$ transition. Notice how the manifold is resolved in CPL spectrum (reproduced with permission from Ref [27]).

Clearly, when this happens, total emission and CPL bands do not coincide in general and special care should be taken in evaluating the g_{lum} value.

Knowing the energies of the *J* levels provides useful information about the crystal field environment which in turn can be correlated with the polarisability of the donor groups.[28]

Often Ln complexes in solution give rise to multiple species of different symmetry and shape which may also be involved in a network of equilibria: in any case the number of lines of each term-to-term manifold cannot exceed the multiplicity of the final state.

In fact, before luminescence occurs, the system rearranges to a single low energy excited state sublevel. If the number of apparent transitions in a given multiplet is larger than expected, this can be taken as a strong indication that there is more than one emitting species.

For example, the observation of a single sharp band for the $^5D_0 \rightarrow {}^7F_0$ transition around 580 nm is often used as an argument in favour of the presence of a single emitting species.

In fact the $^7F_0$ level is non-degenerate and a true single band is expected. However this transition is usually quite weak and the multiplicity can remain hidden within the band width; moreover, owing to the small extent of spin-orbit couplings and the crystal field effects which modulate the exact wavelength of lanthanide *f→f* transitions, accidental degeneracy of the $^5D_0 \rightarrow {}^7F_0$

within several (exchanging) species is possible, which would lead to a true single band in that region.

When dealing with such a situation, it can be convenient to excite the complex with left, right and linearly polarised light; if there is a single emitting species, no significant change of the CPL spectrum will be visible.[29]

Development of complex with high g_{lum} values

Macrocycles and podates

Cyclen (L^1) and its smaller relative triazacyclononane (L^2, Scheme 1) are versatile scaffolds to be functionalised at the N-atoms with arms bearing coordinating groups such as carboxylates, amides, phosphinates and N-donors; central chirality elements can be introduced in the ring or, more frequently, on the side-arms at a carbon centre. [30-33]

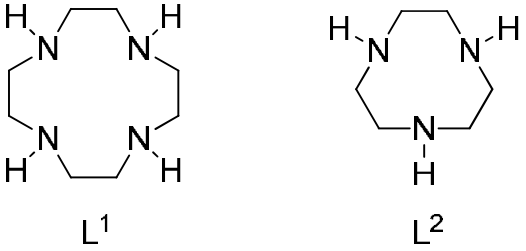

SCHEME 1: Cyclen (L^1) and triazacyclononane (L^2)

The arms can carry also a chromophore (e.g. aryl, etheroaryl, azaxanthones) able to sensitise the lanthanide ion These complexes have been extensively exploited as CPL probes by Parker's group (see Section below).

Podate complexes were shown to strongly bind Ln^{3+} ions, saturating their coordination sphere and shielding them from other coordinating molecules, such as H_2O. This makes them suitable for application in aqueous solutions; water in the first coordination sphere can be a major issue in Ln emission, since O-H is a high-energy oscillator and can lead to a non-radiative deactivation of the luminescence.[34,35]

Raymond et al.[23,25] reported the ligand L^3, in which four 2-hydroxyisophthalamide pendant arms are bound to ethylendiamine; the arms are further functionalised with a 1-phenylethylamine substituent each, encoding the chiral information (Scheme 2).

This ligand has proven to be particularly efficient in sensitising four different Ln^{3+} ions,[iii] namely: Sm^{3+}, Eu^{3+}, Tb^{3+}, Dy^{3+}. All these complexes display good emission and CPL activity. Unfortunately, the geometry and the coordination mode of these complexes remains undetermined.

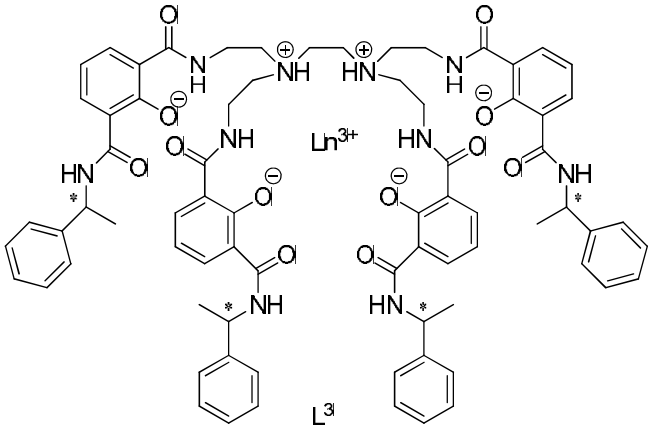

SCHEME 2: Conjectural structure for the podate lanthanide complexes reported by Raymond et al.[23] (Ln=Sm, Eu, Tb, Dy). The stereogenic centers are homochiral and the complex was prepared and characterised with both ligand enantiomers.

The same structural motif was employed to develop similar ligands, designed to provide a bigger steric hindrance and shield the Ln^{3+} ion from water coordination in a more effective way.[37]

β-diketonates

Due to the oxophilicity of Ln^{3+} ions, β-diketonates are effective coordinating molecules for lanthanide ions. Through their use it is possible to prepare *tetrakis* complexes, which are often moisture inert, thanks to the bidentate nature of the ligand: indeed, this leads to an 8-coordination number, and to the fact that the resulting complex is anionic.[iv]

Neutral *tris* species can also be prepared but their coordination sphere must be completed by at least a molecule of water or other Lewis bases such as bipyridines or phenanthrolines.

β-diketonates are often good sensitisers for Eu^{3+}. In particular:

- the diketonate-centred $\pi \rightarrow \pi^*$ transition is strong and falls in the near UV region, moreover its electric dipole moment is centred in the middle of the diketonate moiety;
- Eu^{3+} ion is only 2.3–2.4 Å distant from the donor oxygen atoms[v, 11]
- substituents at 1 or 3 positions can modify the absorption wavelength of the diketonate and modulate the energy of the triplet state, in order to optimise the energy levels involved in the ligand-to-metal energy transfer;
- chiral diketones can be easily synthesised through a Claisen type reaction from cheap natural enantiopure ketones.

Therefore, it is not surprising that many complexes with outstanding optical and chirooptical properties belong to this class: to the best of our knowledge, $Eu(TTA)_3 2L^6$ (TTA = 2-thenoyltrifluoroacetonate, L^4; L^5 = dibenzylsulfoxide; Scheme 3) displays the highest quantum yield reported for an Eu^{3+} complex (85%) at solid state,[39,40] while the heterobimetallic complex $CsEu(hfbc)_4$ (hfbc = heptafluorobutyrylcamphorate, L^6; Scheme 3) showed a g_{lum} value of 1.38, the highest ever measured for a Ln^{3+} system.[20,24] It should also be noted that the same ligand L^6 was able to sensitise Sm^{3+}, providing another complex with excellent polarisation characteristics. For the manifold associated to the Sm^{3+} $^4G_{5/2} \rightarrow {}^6H_{5/2}$ transition, Kaizaki et al.[24]

[iii] It may be interesting to notice that the same ligand was also employed to sensitise curium(III).[36]

[iv] It should be recalled that LnDOTA complexes are partially hydrated, despite the fact that the ligand is 8-dentate and the resulting complexes anionic. However, this is a function of the ionic radius of a given lanthanide.[38]

[v] Two main mechanisms describe the energy transfer: *Dexter* and *Förster resonant energy transfer* (FRET).[2] Both depend strongly on the donor-acceptor distance *R*: Dexter mechanism depends on $e^{-\alpha R}$, while FRET depends on R^{-6}.

Reported g_{lum} values of -1.15 (at 553 nm), -0.35 (561 nm), +0.96 (575 nm) and -0.45 (588 nm).

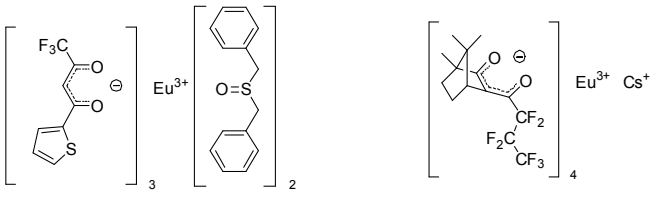

$Eu(TTA)_32L$ $CsEu(hfbc)_4$

$EuL^4{}_32L^5$ $EuL^6{}_4$

SCHEME 3: Two Eu^{3+} complexes displaying peculiar optical ($Eu(TTA)_32L^5$, quantum yield=85 %), and chirooptical ($CsEu(hfbc)_4$, g_{lum} = 1.38) features.

Camphor-based systems

Camphor provides a rigid chiral backbone employable in the synthesis of β-diketones; aside from the exceptional performances already mentioned for $CsEu(hfbc)_4$, several other camphorate-based complexes have been investigated by CPL spectroscopists with interesting results.

Tris europium trifluoromethylcamphorate ($Eu(facam)_3$, facam=L^7; Scheme 4) in dimethylsulphoxide displays a g_{lum} of |0.78|[41] and it is used as a standard for CPL instruments calibration,[42] even though this practice has been recently criticized and other systems have been proposed.[43]

Recently $Eu(facam)_3$ complexes with several ancillary ligands have been synthesised and their CPL measured in solution.

Harada et al.[44,45] have employed ligands with *atropos* or *tropos* axial chirality such as (*R*/*S*)-2,2'-bis(diphenylphosphoryl)-1,10-binaphthyl ((*R*/*S*)-BINAPO, (*R*/*S*)-L^9), 2,2'-bis(diphenylphosphoryl)-1,10-biphenyl (BIPHEBO, L^{10}), with central chirality as bis-(4*R*/4*S*)-(4-isopropyl-oxazolinyl)pyridine ((*R/S*)-^{i}Pr-Pybox, ((*R/S*)-L^{11}), and bis-(4*S*,5*S*/4*R*,5*R*)-(4-methyl-5-phenyl-oxazolinyl)pyridine ((*S*,*S*/*R*,*R*)-Me-Ph-Pybox, (*S*,*S*/*R*,*R*)-L^{12}), and achiral ligands as 1,10-phenanthroline (Phen, L^{13}) and triphenylphosphine oxide (TPPO, L^{14}) (Scheme 4). The reported g_{lum} values for the magnetic transitions in acetone-d_6 range from |0.44| to |1.0| (Table 2).

Changing the absolute configuration of the ancillary ligands in Eu((*R*/*S*)-BINAPO)(*D*-facam)$_3$ and Eu((*R*/*S*)-^{i}Pr-Pybox)(*D*-facam)$_3$, the g_{lum} sign remains unchanged, indicating that in these cases the CPL activity is mainly controlled by the chirality of *D*-facam ligands.

TABLE 2 Ancillary ligands for Eu(*D*-facam)$_3$ and g_{lum} values of the resulting complexes measured in d_6-acetone[44,45] (see Scheme 4).

Ancillary ligand	g_{lum} (λ=595 nm)
(*R*)-BINAPO ((*R*)-L^9)	0.44
(*S*)-BINAPO ((*S*)-L^9)	0.34
BIPHEBO (L^{10})	0.24
(*R*)-^{i}Pr-Pybox ((*R*)-L^{11})	-1.0
(*S*)-^{i}Pr-Pybox ((*S*)-L^{11})	-0.8
(*S*,*S*)-Me-Ph-Pybox (*S*,*S*)-L^{12})	-1.0
Phen (L^{13})	-0.46
TPPO (L^{14})	0.47

Other diketonate-based chiral complexes

1,1,1,5,5,5-hexafluoropentane-2,4-dione (HFA, L^8, Scheme 4) is known to be a good sensitiser for Eu^{3+}. HFA has been used by Yuasa et al.[46] to synthesise a series of complexes $Ln(HFA)_3L^*$ (L*=L^{15}, L^{11}, L^{12}, Scheme 4) in which the chiral ligand L* induces an asymmetric arrangement of the three HFA ligands around the lanthanide.

With the reported series of Pybox ligands as L*, they obtained high luminescence quantum yields (34–41%) and g_{lum} values (|0.15|–|0.46|) in CD_3CN solution for Eu^{3+} complexes.

Interestingly enough, the signs of the $^5D_0 \rightarrow {}^7F_1$ and $^5D_0 \rightarrow {}^7F_2$ transitions were the same for L*=(*R*)-^{i}Pr-Pybox ((*R*)-L^{11}) and (*R*,*R*)-Me-Ph-Pybox ((*R*,*R*)-L^{12}) but they were inverted for bis-4*R*-(4-phenyl-oxazolinyl)pyridine ((*R*)-Ph-Pybox, (*R*)-L^{15}) (see Table 3 and Scheme 4).

In order to correlate the CPL spectrum signature with the complex structure, single-crystal X-ray structural analyses were performed. It was found that the ligand-ligand intramolecular interactions account for the asymmetric arrangement around the lanthanide ion, justifying the observed CPL spectrum signature. Anyway no analysis to assess the actual structure in solution neither the possible stereoisomer equilibria was carried out. However, the CD spectra measured in solution for $EuL^8{}_3L^{11}$ and $EuL^8{}_3L^{12}$ display bands with the same sign, while the sign it is inverted for $EuL^8{}_3L^{15}$, consistently with the solid state data.

It is worth noting that the CPL of $Eu(facam)_3L^{14}$ and $Eu(HFA)_3L^{15}$ has been investigated even at solid state taking the measurement on single crystals.[47]

TABLE 3 Ancillary ligand for $Eu(HFA)_3$ and g_{lum} values of the resulting complexes measured in CD_3CN[46] (see Scheme 4).

Ancillary ligand	g_{lum}	
	$^5D_0 \rightarrow {}^7F_1$	$^5D_0 \rightarrow {}^7F_2$
(*R*)-Ph-Pybox ((*R*)-L^{15})	0.15	-0.020
(*R*)-^{i}Pr-Pybox ((*R*)-L^{11})	-0.46	0.034
(*R*,*R*)-Me-Ph-Pybox ((*R*,*R*)-L^{12})	-0.35	0.026

Polynuclear systems

Recently, chiral polylanthanidic systems with large g_{lum} values have begun being synthesised.

Mamula et al.[48] reported a C_3 trinuclear complex with a chiral bipyridine–carboxylate ligand (L^{16}, Figure 2), formed through a completely diastereoselective self assembly process which shows also a complete chiral self-recognition in the presence of enantiomer mixtures of the ligand, yielding the system of formula $Eu_3L^{16}{}_6$. In addition ^{1}H-NMR studies showed that the gross crystal structure of the system (see Figure 2) is preserved in CH_2Cl_2 solution.[4] g_{lum} of |0.088| and |0.0806| were measured in CH_2Cl_2 for the $^5D_0 \rightarrow {}^7F_1$ and $^5D_4 \rightarrow {}^7F_5$ transitions of the Eu^{3+} and Tb^{3+} complexes respectively.

More recently, Mazzanti et al.[10] syntesised an Eu^{3+} complex with multilayered supramolecular architecture using (S/R)-6'-(4-phenyloxazolin-2-yl)-2,2'-bipyridine-6-carboxylate as a ligand (L^{17}, Figure 3) and investigated its optical properties.

Starting from a ligand of *S* (or *R*) chirality, one obtains a mixture of diastereomeric Δ and Λ complexes of $EuL^{17}{}_2$ stoichiometry with only partial selectivity (Λ/Δ≈1.8, with *S* ligand). In concentrated acetonitrile solution (6 mM), complexes of formula $Eu_3L^{17}{}_6$ self-assemble with a defined helicity (namely Δ, with *S* ligand), this system display 25% quantum yield with a |0.45| g_{lum} value for the $^5D_0 \rightarrow {}^7F_1$ transition.

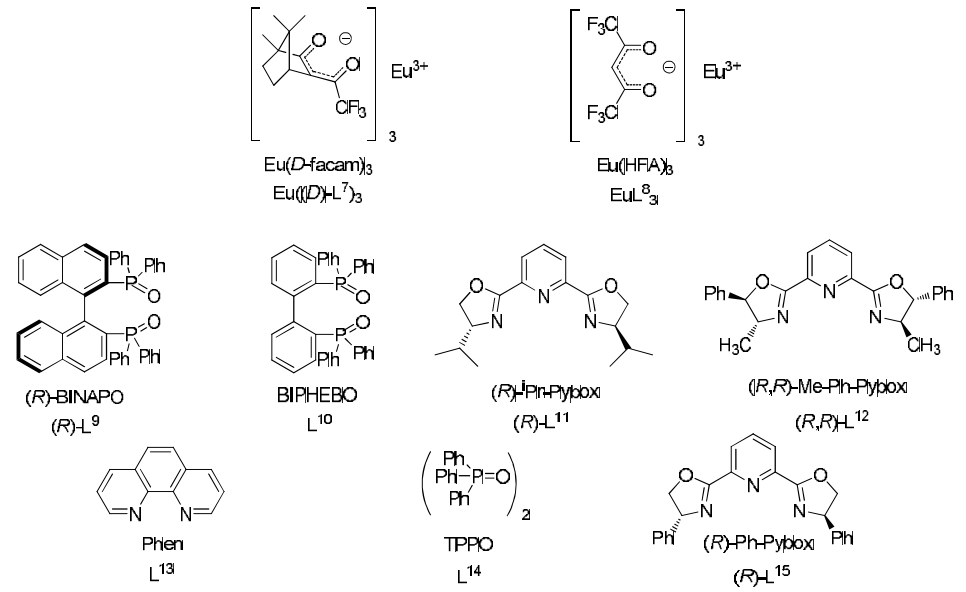

SCHEME 4: Diketonate-based Eu^{3+} complexes and ancillary ligands reported in References [44-46].

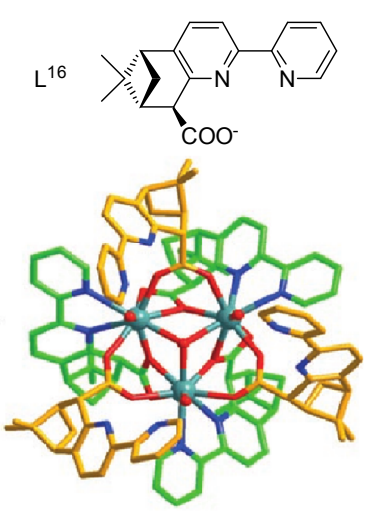

FIGURE 2: (–)-5,6-pinene-bipyridine ligand (L^{16}) and the X-ray structure of the $(EuL^{16}_2)_3$ complex (reproduced with permission from Ref [4]).

A controlled addition of $Eu(OTf)_3$ leads to formation of an heptanuclear system displaying a 27% quantum yield with a |0.10| g_{lum} value. This g_{lum} is lower than that measured for the trinuclear complex, in fact in the heptanuclear system, a central Eu^{3+} ion coordinates six EuL^{17}_2 units; six of them display Δ chirality, while the other six ones display Λ chirality; moreover these units come in an alternate fashion, so the intrinsic chirality of each EuL^{17}_2 is almost balanced out in the complex (Figure 3).

Lanthanide CPL probes for molecular sensing

Thanks to the great sensitivity of the CPL signals to conformational and structural aspects and to the peculiar optical and chirooptical properties discussed above, lanthanide complexes have been employed as probes for small molecules and also proteins.

Parker et al. reported a wealth of cyclen and triazacyclenonane-based Eu^{3+} and Tb^{3+} complexes[9,49-51] (Scheme 1).

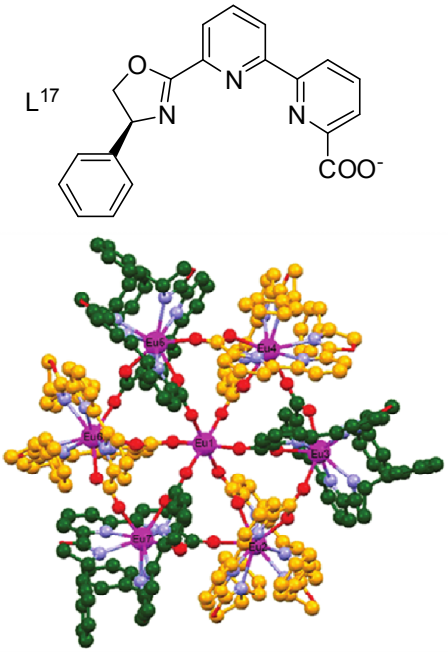

FIGURE 3: Top: (*S*)-6'-(4-phenyloxazolin-2-yl)-2,2'-bipyridine-6-carboxylate (L^{17}) ligand. Bottom: the XRD structure of the heptanuclear complex, where the units yellow and green represent Δ and Λ mononuclear complexes EuL^{17}_2, respectively (reproduced with permission from Ref [10]. Copyright 2012 American Chemical Society).

Lanthanide CPL and organic molecules

Dynamically racemic complexes

Tb^{3+} *tris* 2,6-pyridine-dicarboxylate (L^{18}) and chelidamic acid (L^{19}) (Scheme 5) D_3 racemic complexes can interact with non racemic compounds, giving rise to CPL.[52,53] Recently, they have been employed by Muller et al.[54] as probes for aminoacids. These are in fact chiral D_3 complexes, but Λ and Δ enantiomers undergo a rapid equilibrium in solution and can not be resolved.

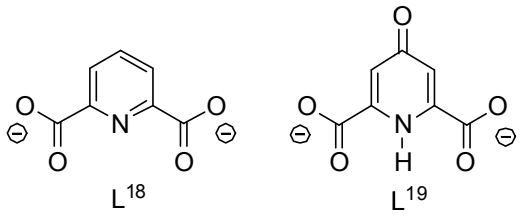

L^{18} L^{19}

SCHEME 5: 2,6-pyridine-dicarboxylate (L^{18}) and chelidamic acid (L^{19}).

When they interact with enantiopure aminoacids, thanks to their ability to form a hydrogen-bond network, one form prevails over the other one, since they are now in a diastereomeric relationship (*Pfeiffer effect*).[55,56] This event is signalled by the rising of an induced CPL signal in the region of the $^5D_4 \rightarrow {}^7F_5$ transition.

With a similar approach, Parker et al. syntesised a cyclen-based Eu^{3+} (EuL^{20}) complex in which the chirality of the complex is defined by the position of the azaxanthone and carboxylate pendant arms but it is dynamically racemic and of course no CPL can be detected (Figure 4).[50,57]

When α_1-acid glycoprotein (α_1-AGP) is added, EuL^{20} shows optical activity and a CPL signal is switched on. The complex is coordinatively unsaturated and a weakly coordinated axial water molecule is needed to fill the coordination sphere.

The α_1-AGP displaces the axial ligand and, at the same time, it perturbs the racemic equilibrium towards one of the two conformational enantiomers, as signalled by the change of the total emission spectrum and mainly by the appearance of a strong CPL signal (Figure 4).

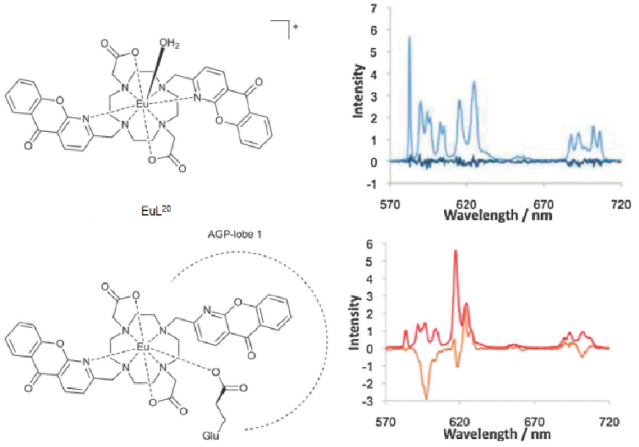

FIGURE 4: Binding between the EuL^{20} and α_1-AGP. On the right: CPL (blue navy and orange) and total luminescence (light blue and red) for free and bound forms (reproduced from Ref [50] with permission of The Royal Chemical Society).

In particular the g_{lum} factor of the $^5D_0 \rightarrow {}^7F_1$ transition increases upon adding the protein, allowing one to estimate a binding constant for the system formed by EuL^{20} and α_1-AGP.

Given the selectivity of the CPL response to α_1-AGP, this one and similar systems pave the way to the development of an analytical method to track this protein: the importance of monitoring α_1-AGP levels in serum has been recently recognised, because it increases as a response to an inflammatory acute state and can be used as a biomarker for breast cancer.

Enantiopure complexes

Enantiopure complexes are endowed with intrinsic CPL, which can be modified in both intensity and shape after the interaction with a target molecule.

The CPL signal accompanies total luminescence and provides an additional information, since the shape and signature of the CPL spectrum is very sensitive to the coordination environment and thus the signal may be very specific for a certain target.

Parker et al. reported Tb^{3+} and Eu^{3+} enantiopure cyclen-based systems as CPL probes for proteins:[9] Figure 5 shows the Tb^{3+} macrocyclic complex TbL^{21} employed for serum albumin sensing.[58]

The complex bears three asymmetric carbon atoms on the side-arms and it exists as diastereomer pair: *SSS*-Δ-[TbL^{21}] and *SSS*-Λ-[TbL^{21}] with the former being prevailing in solution.

Serum albumin binds to *SSS*-Δ-[TbL^{21}] (and only more weakly to its enantiomer), and as a consequence to the formation of this adduct, the preferred helicity of TbL^{21} is reversed from Δ to Λ and a switching of the CPL spectrum signature is observed.[59]

This switching occurs selectively with serum albumin while it does not with other proteins, cyclodextrins or chiral anions. This led Parker et al. to envisage a potential use for these complexes as a probe for circularly polarised luminescence microscopy.[9]

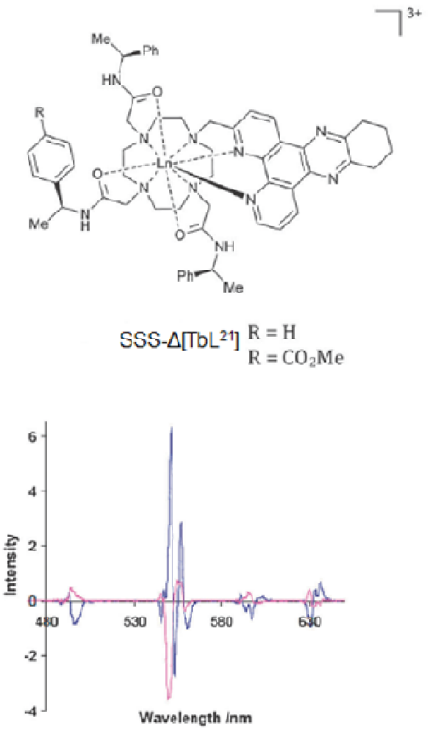

FIGURE 5: Lanthanide macrocyclic complex (TbL^{21}) and CPL spectrum before (blue) and after (purple) addition of serum albumin (reproduced with permission from Ref [9]. Copyright 2009 American Chemical Society).

The sensitive nature of the lanthanide-centred CPL has been further demonstrated by Yuasa et al.[8] A 1-biphenyl-3-perfluoroethyldiketonate moiety was covalently bound to bovine serum albumin or other proteins, such as *Staphylococcus aureus* recombinant nuclease A and insulin. This diketonate has a strong affinity for lanthanides and is a good sensitiser for Eu^{3+}; in fact, complexing these systems with Eu^{3+}, the protein fills the coordination sphere around the lanthanide as a function of its structural and chemical characteristics, in addition, it provides an asymmetric environment allowing one to record different Eu^{3+}-centred CPL spectra (Figure 6).

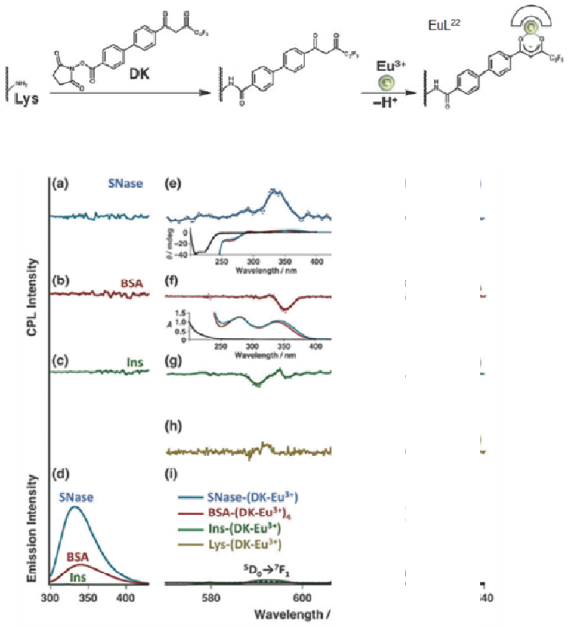

FIGURE 6: Covalent binding of 1-biphenyl-3-perfluoroethyldiketonate to the protein and complexation with Eu^{3+} and Eu-centred CPL of various adducts (reproduced from Ref [8] with permission of The Royal Chemical Society).

Lanthanide CPL and ion binding

Lanthanides display strong affinity for hard anions, which are able to displace weak neutral ligands. Moreover it is possible to tune the coordination strength of acidic ligands as a function of pH and the pK_a of the ligand itself. A variable coordination may modulate the coordination geometry to which CPL is sensitive.

Eu^{3+} complexes have been used as probes for bicarbonate or pH.[50,60] Various enantiopure cyclen-based structures have been developed as responsive systems in which the concentration of bicarbonate can be tracked following the variation of the luminescence dissymmetry factor for a selected transition.

Complex EuL^{23}, bearing a sulfonamide moiety on one arm has proven to be pH-responsive: when pH increases the sulfonamide moiety is deprotonated and thus it is able to coordinate the metal centre; this results in a rigidification of the complex leading to increasing g_{lum} values at 632 nm (Figure 7).

According to Parker et al.,[50] it is also possible that the coordination changes the geometry around the lanthanide providing a twist angle closer to the ideal one for static coupling mechanism (namely 22.5°) (see Section below).

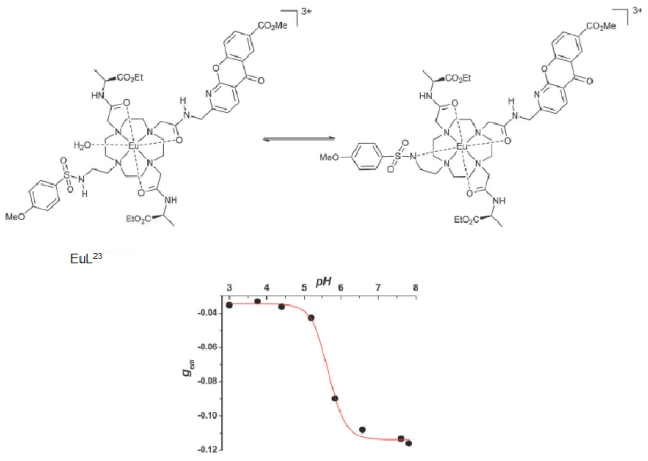

FIGURE 7: Top: changes in the coordination sphere of EuL^{23} as a response to increasing pH. Bottom: g_{lum} for the transition at 632 nm as a function of pH (reproduced from Ref [50] with permission of The Royal Chemical Society).

Origin of strong CPL

Any chirooptical activity requires a non-vanishing rotational strength:

$$R_{ij} = \Im\left[\left\langle i\left|\hat{\boldsymbol{\mu}}\right|j\right\rangle \cdot \left\langle j\left|\hat{\mathbf{m}}\right|i\right\rangle\right] = \Im\left[\boldsymbol{\mu}_{ij} \cdot \mathbf{m}_{ji}\right] \qquad (4)$$

where $\hat{\boldsymbol{\mu}}$ and $\hat{\boldsymbol{m}}$ are the electric and magnetic dipole transition operators and $\Im$ is the imaginary part of the following expression. In an emission process the energy of the initial state *i* is higher than that of the final state *j*; in this case equation (4) gauges CPL.

For a magnetic dipole allowed-electric dipole forbidden transition, like a Ln-centred f-f transition, $\boldsymbol{\mu}_{ij} \approx 0$[vi] is expected and therefore a vanishing rotational strength. The process giving rise to CPL activity can be conveniently represented with reference to two limiting mechanisms: *static* and *dynamic coupling*.[22] The former is the only possibly relevant when the ligand lacks any significant chromophoric group; in all the other cases both mechanisms should be taken carefully into account.

Static coupling

In a dissymmetric environment, a mixing of e.g. *4f* and *5d* orbitals may provide the necessary odd-parity interconfigurational character yielding $\boldsymbol{\mu}_{ij} \neq 0$ [22,61]. This can happen only if the first coordination sphere is chiral and therefore the covalent contribution to the bonds between the lanthanide and the donor atoms entails invoking such hybrids.

In the typical parlance of the chirooptical spectroscopies, and in particular in ECD, this case can be described as an intrinsically chiral chromophore.

In the limit of low covalence, the coordination neighborhood causes only a weak perturbation to the metal states, so the sum rule can apply yielding a vanishing integral of the CD or CPL spectrum over all the *f* transitions. This is hardly of practical aid when we deal with a complex of Eu^{3+}, Tb^{3+} or other visible-emissive lanthanides, because their transitions range from IR to UV region and many of them will almost surely be covered by ligand-centred bands.

Yb^{3+} and Ce^{3+} represent a special case: since they have a $4f^1$ and $4f^{13}$ electronic configuration respectively, they behave as

vi We recall that $\boldsymbol{\mu}_{ij}$ is exactly 0 only in a centro-symmetric environment, however even for chiral molecules it is generally very small.

monoelectronic systems with only two levels each. In particular, while Ce^{3+} $^2F_{7/2} \rightarrow {}^2F_{5/2}$ transition falls in the IR region and may be covered by ligand VCD signals; Yb^{3+} $^2F_{7/2} \rightarrow {}^2F_{5/2}$ falls in the NIR region and can thus be often easily recorded without significant interferences.[32,62] In the limit of perfect static coupling the integral over the manifold corresponding to the M_J splitting allied with this transition is expected to vanish.

This result can be transferred to isostructural complexes of other lanthanides. Lanthanide complexes often show isostructurality along the series; this means that the geometry of the system may show no significant dependence on the lanthanide ion.[vii]

For this mechanism, in the common case of a distorted square antiprismatic geometry, as found for example in DOTA-like complexes or in *tetrakis* diketonates (notably in the case of $CsEuL^6_4$) the CPL signal should vary with the *twist angle* φ following a $\sin(4\varphi)$ trend, so the maximum is reached for φ=22.5° (Figure 8).[64]

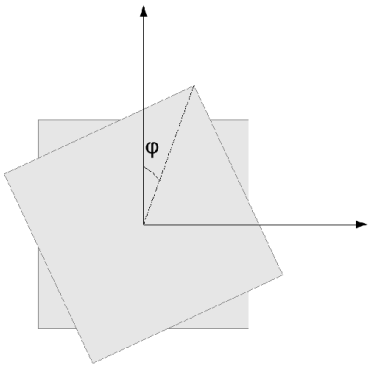

FIGURE 8: Twist angle φ in the case of a distorted square antiprismatic geometry.

Dynamic coupling

When the coordination polyhedron is itself achiral, the ligand field should allow only for *f*→*f* electronic transitions with pure magnetic dipole character. Once more, making reference to common nomenclature in ECD theory, we deal with an intrinsically achiral chromophore. Optical activity can stem from some coupling interaction between metal-centered transitions and the dissymmetric environment provided by the ligands beyond the first coordination sphere.

The previously cited $CsEu(hfbc)_4$ (Scheme 3) complex provides an interesting example to analyse.

$CsEu(hfbc)_4$ has an almost perfect antiprismatic geometry in solution with a twist angle of -41.4°, thus static coupling mechanism alone can not account for the measured g_{lum}=1.38 value at 598 nm,[65] i.e. for the $^5D_0 \rightarrow {}^7F_1$ transition, which has magnetic dipole but no electric dipole character. Indeed, in an ideal antiprismatic geometry the twist angle is 45°, which means that the coordination polyhedron is completely symmetric with respect to rotoreflection operations.

On the other hand, dynamic coupling between the Eu-centred and the nearby diketonate $\pi \rightarrow \pi^*$ transitions may help us rationalising this case.

Figure 9 represents two of the 4 β-diketonate moieties of the $CsEu(hfbc)_4$ complex (belonging to C_4 point group).

The lanthanide-centred $^5D_0 \rightarrow {}^7F_1$ magnetic transition ($\boldsymbol{m}_{Ln}$) is associated with electric quadrupole moment; the nearby diketonate groups constitute polarisable linear oscillators ($\boldsymbol{\mu}_{lig}$), which can be excited (through dipole-quadrupole interaction) when the $^5D_0 \rightarrow {}^7F_1$ transition is active, providing a $\boldsymbol{m}$-$\boldsymbol{\mu}$ coupling mechanism.[66]

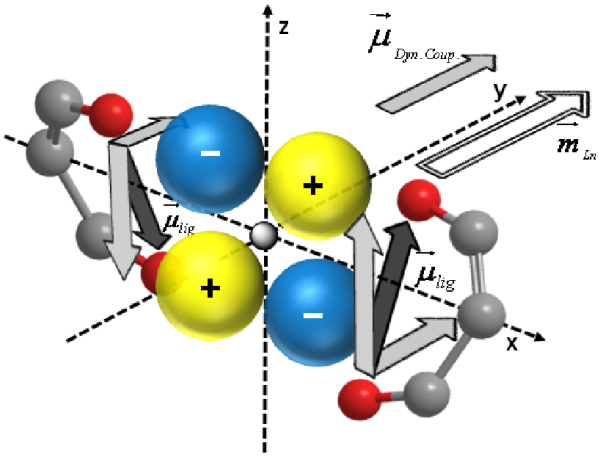

FIGURE 9: Dynamic coupling mechanism occurring in a C_4–symmetric Ln diketonate: for simplicity, only two β-diketonate moieties are depicted. The four lobes represent the quadrupolar charge distribution (blue and yellow) allied to the magnetic dipole transition (with moment $\boldsymbol{m}_{Ln}$, along the *y*-axis). This induces a polarisation of the diketonate group, which is represented by the two skew $\boldsymbol{\mu}_{lig}$ vectors. The horizontal components of $\boldsymbol{\mu}_{lig}$ provide non vanishing terms to the scalar product $\boldsymbol{m}\cdot\boldsymbol{\mu}$. (Adapted from Ref [67]).

With reference to Figure 9, the lanthanide-centred magnetic moment $\boldsymbol{m}_{Ln}$ (belonging to irrep *E* of the C_4 point group) is contained in the *x*-*y* plane, orthogonal to the C_4 (*z*-axis). For the sake of simplicity, in Figure 9 we represented only its *y*-component. The associated quadrupolar charge distribution during this Ln-centered transition is shown as well.

Each diketonate can be depicted as a linear polarisable group, directed parallel to the vector joining the two oxygen atoms, that is, oblique with respect to the *xy*-plane. When the Ln-centred transition is excited (either in absorption or in emission), its associated electric quadrupole induces a simultaneous electric dipole moment $\boldsymbol{\mu}_{lig}$ on each diketonate. In turn, these 4 electric dipoles couple with one another providing components with different symmetry: either belonging to *A*-irrep, *i.e.* oriented along *z*, or doubly degenerate (*E*) in the *x*-*y* plane.

Only this latter (low energy) *E* component of the $\boldsymbol{\mu}_{lig}$ -$\boldsymbol{\mu}_{lig}$ coupling ($\boldsymbol{\mu}_{Dyn.Coup}$) can constructively interact with the $\boldsymbol{m}_{Ln}$ to provide rotational strength (consisting in the scalar product $\boldsymbol{m}\cdot\boldsymbol{\mu}$). On the contrary, the axial *A*-counterpart leads to cancellation.

Dynamic coupling mechanism can only be efficient when the lanthanide and the chromophoric group are spatially close, since the dipole-quadrupole interaction depends on the Ln-$\boldsymbol{\mu}_{lig}$ distance R^{-4}; moreover it depends on the difference between the frequencies of the lanthanide-centred and the ligand-centred transitions; this dependence can be accounted for as a perturbation. When these conditions are fulfilled, this mechanism can provide transitions with a strong circular polarisation, if compared with the simple static coupling; in fact dynamic coupling does not entail invoking Ln orbital hybridation, which is generally small, since the covalency is low in the Ln-ligand bond.

When this mechanism is active, *f*→*f* transitions can no longer be considered isolated, because it is naturally coupled with ligand-centred transition(s); so, unlike the case of static coupling, the integral over the bands of the NIR-CD spectrum of an Yb^{3+} isostructural complex will be non-vanishing.

vii Ligand-centred ECD spectra of isostructural compounds do not display significant variations. A non-chirooptical method to asses isostructurality is through analysis of the NMR data; in fact paramagnetic shifts and relaxation rates of paramagnetic Ln^{3+} compounds contain geometric information. For details we refer to the specific literature.[62,63]

Suggestions on how to measure and report CPL spectra of lanthanide complexes

CPL spectra are measured through a continuous wave scan whose most significant parameters are the passing band *w*, the time constant *k* and the scan speed *v*; they all display critical aspects, when dealing with Ln complexes.

A general rule among spectroscopists states that these parameters must fulfill the condition:

$$\frac{1}{2}w > k \cdot v \qquad (5)$$

Particular caution should be taken in setting the passing band width; in fact, as stated above, lanthanide emission bands can be very narrow (less than 5 nm), and they are often multiplets with nearby bands, with possibly opposite CPL sign; if this components remain unresolved, they will cancel out (at least partially), causing error in the assessment of the intensity of the CPL signal and in the calculation of the g_{lum} value.

With a passing band of 1 nm and a time constant of 1 sec, the scan speed should be set to 0.5 nm/sec. As an example we note that it will take 4 min for each scan to a acquire 120 nm region: this may be typical when dealing with Eu^{3+} complexes.

A low enough scan speed is also necessary to accurately detect the emission maxima of the narrow CPL lines, which in turn is necessary to calculate accurate g_{lum} values.

Lanthanide CPL spectra are usually recorded with a 90° geometry between the source and the detector, as in an ordinary fluorescence experiment. On the other hand, if it were an issue, their large Stokes shift would allow one to adopt an in-line geometry. To this end, one must prevent the exciter beam to reach the detector, which may be achieved by simply adding a low-pass filter after the sample. When using a diffraction-grate monochromator, one must be aware that higher harmonics of the exciting radiation may fall in the emission region.[viii]

Moreover, the large luminescence dissymmetry factors usually obtained for lanthanides, may allow one to measure lanthanide CPL spectra using simple static optics, employing a quarter wave retarder and a linear polariser. Early measurements in the field of CPL were made with similar devices without photoelastic modulators, which are now common in CPL spectrophotometers.[68]

This setup allowed Oosterhoof et al. to measure g_{lum} values with a standard deviation within 0.005 and 0.01.[69-71]

More about the luminescence dissymmetry factor

Plotting g_{lum} vs. λ

In a CPL measurement ΔI and I are not absolute quantities, in fact, as in ordinary fluorescence experiments, not all of the emitted light is detected, depending on the experimental conditions. On the other hand, the luminescence dissymmetry factor, as defined in equation (1), is an absolute value. Therefore there are good physical reasons to discuss and report CPL spectra in terms of g_{lum}, not only of individual bands but also as a continuous function of wavelength (or wavenumber).

However some precautions should be taken when plotting g_{lum} (λ).

Indeed, out of the emission zones, I and ΔI are equal to 0, thus g_{lum} gives rise to a mathematically undefined form: the practical result is an amplification of the instrumental fluctuations around zero emission,[ix] with erratic and possibly very large values of g, where one would actually expect 0. This may be quite a serious issue with lanthanides, since the emission bands are very narrow and commonly without relevant tailing. Moreover, such narrow bands are commonly instrumentally traced with very few data points, therefore trying to eliminate the noise through smoothing algorithms is a risky choice, in fact in this way a faithful reproduction of the profile of these bands can be hard to achieve.

We therefore suggest to introduce a trivial mathematical artifice defining a *corrected* g_{lum} as

$$\tilde{g}_{lum} == \frac{\Delta I}{I + \delta} \qquad (6)$$

where the correcting constant δ has to be chosen bigger than the instrumental noise but negligible with respect to the smallest emission signal one wants to measure (for example, 1/100 of I).

As an example, in Figure 10 we show a plot of g_{lum} (without correction) and $\tilde{g}_{lum}$ (δ=3·10^{-4}, i.e. 2/100 of the maximum intensity of the band at 585 nm) for a CPL spectrum obtained for $CsEu(hfbc)_4$.

For instance, considering the 550–570 nm region, one can see that the correction is sufficient to smooth the baseline while not large enough to significantly affect the signal bands (Insets of Figure 10).

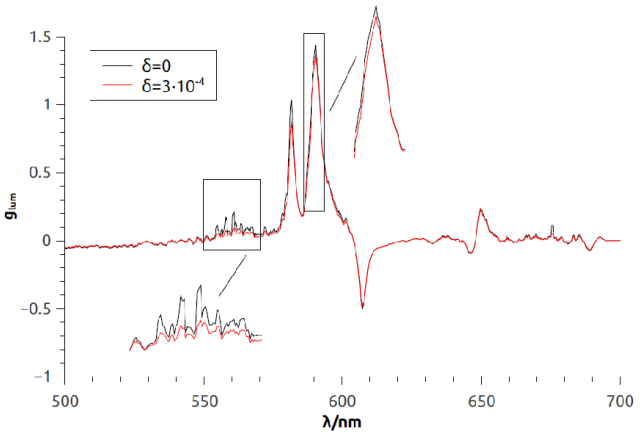

FIGURE 10 Plot of g_{lum} with (red) and without correction (black) for $CsEu(hfbc)_4$. Notice that the baseline is smoothed while the bands are not affected by the correction (insets). The CPL and emission spectra for generating this plot were recorded on the instrument described in ref. [68].

Instrumental error on g_{lum}

Since the pulses due to incident light onto the detector follow Poisson statistics, the associate standard deviation is $\sqrt{N}$, where N is the total number of photon counts. The standard deviation on $\Delta I = I_L - I_R$ is $\sigma_{\Delta I} = \sqrt{2N}$, while on $I = 1/2\,(I_L + I_R)$, it is $\sigma_{I_{TOT}} = \sqrt{\frac{N}{2}}$. To derive the standard deviation $\sigma_{g_{lum}}$ on g_{lum}, we have to solve:[x]

$$\sigma_{g_{lum}} = \sqrt{\left[\frac{\partial g_{lum}}{\partial \Delta I}\right]^2 \sigma_{\Delta I}^2 + \left[\frac{\partial g_{lum}}{\partial I}\right]^2 \sigma_I^2} \qquad (7)$$

that is:

$$\sigma_{g_{lum}} = \frac{\sqrt{N}}{\sqrt{2}I}\sqrt{4 + g_{lum}^2} \qquad (8)$$

Considering I proportional to N, we get:

---

viii For example setting the excitation to 305 nm, it may interfere with the 610 nm band of an Eu^{3+} complex.

ix This noise comes from the definition of g_{lum} itself and not directly from the experimental measurement.

x We should note that here we are neglecting the term containing the covariance: $\left[\frac{\partial g_{lum}}{\partial \Delta I} \cdot \frac{\partial g_{lum}}{\partial I}\right] \sigma_{\Delta I, I}$.

$$\sigma_{g_{\mathrm{lum}}} = \frac{1}{\sqrt{2N}}\sqrt{4+g_{\mathrm{lum}}^2} \quad (9)$$

If g^2_{lum} is negligible with respect to 4, we obtain the expression generally reported:[41]

$$\sigma_{g_{\mathrm{lum}}} = \sqrt{\frac{2}{N}} \quad (10)$$

Otherwise, as is often the case with lanthanide CPL, $\sigma_{g_{\mathrm{lum}}}$ does depend on the g^2_{lum} value itself.

Perspectives and concluding remarks

Chemists may design and synthesise new ligands in order to optimise the desirable properties of the final lanthanide complex. In particular an optimal ligand should:

- form a stable/inert lanthanide complex;
- be a good sensitiser for a given lanthanide;
- form a complex with a chiral geometry that can give rise to a strong CPL, according to the mechanisms described herein;
- form a complex with good solubility in the intended solvent or medium.

Lanthanide peculiar spectroscopic features (large Stokes shift, narrow and characteristic emission bands), joined with their outstanding circularly luminescence properties can give rise to a multidisciplinary interest. The selectivity of the CPL response is employed as a bioanalytical method to quantify and track biomarkers, and more specific tools, as circularly polarised microscopy, can be developed using tailored lanthanide complexes.[1,9]

Other applications, in which luminescent lanthanide complexes are already employed, can be extended using chiral analogues with strong circularly polarised emission, this may include, for example, the development of electroluminescent circularly polarised light emitters.

Another asset worth to be employed is the luminescence of different lanthanides extending to near infrared (NIR) region; this would allow one to obtain molecules with circularly polarised emission in a region that can not be easily reached with chiral organic emitters. However, so far, only few pioneristic works concerning the measurement of CPL in the NIR region have been reported,[72-74] therefore it remains a relatively novel field to explore.

Acknowledgments

Financial support from MIUR-PRIN 2012A4Z2RY is gratefully acknowledged. We wish to thank Prof.s S. Abbate and G. Longhi and Dr. E. Castiglioni for recording the spectra of $CsEu(hfbc)_4$.

Literature Cited

1. Moore EG, Samuel APS, Raymond KN. From Antenna to Assay: Lessons Learned in Lanthanide Luminescence. Acc Chem Res 2009;42:542-552.
2. Bunzli J-CG, Piguet C. Taking advantage of luminescent lanthanide ions. Chem Soc Rev 2005;34:1048-1077.
3. Bunzli J-CG, Eliseeva SV. Intriguing aspects of lanthanide luminescence. Chemical Science 2013;4:1939-1949.
4. Lama M, Mamula O, Kottas GS, Rizzo F, De Cola L, Nakamura A, Kuroda R, Stoeckli‐Evans H. Lanthanide class of a trinuclear enantiopure helical architecture containing chiral ligands: Synthesis, structure, and properties. Chemistry-A European Journal 2007;13:7358-7373.
5. Piguet C, Bünzli J-CG, Bernardinelli G, Hopfgartner G, Petoud S, Schaad O. Lanthanide Podates with Predetermined Structural and Photophysical Properties: Strongly Luminescent Self-Assembled Heterodinuclear d−f Complexes with a Segmental Ligand Containing Heterocyclic Imines and Carboxamide Binding Units. J Am Chem Soc 1996;118:6681-6697.
6. Klink SI, Keizer H, van Veggel FCJM. Transition Metal Complexes as Photosensitizers for Near-Infrared Lanthanide Luminescence. Angew Chem Int Ed 2000;39:4319-4321.
7. Pope SJA, Coe BJ, Faulkner S, Bichenkova EV, Yu X, Douglas KT. Self-Assembly of Heterobimetallic d−f Hybrid Complexes: Sensitization of Lanthanide Luminescence by d-Block Metal-to-Ligand Charge-Transfer Excited States. J Am Chem Soc 2004;126:9490-9491.
8. Yuasa J, Ohno T, Tsumatori H, Shiba R, Kamikubo H, Kataoka M, Hasegawa Y, Kawai T. Fingerprint signatures of lanthanide circularly polarized luminescence from proteins covalently labeled with a β-diketonate europium (iii) chelate. Chem Commun 2013;49:4604-4606.
9. Montgomery CP, Murray BS, New EJ, Pal R, Parker D. Cell-Penetrating Metal Complex Optical Probes: Targeted and Responsive Systems Based on Lanthanide Luminescence. Acc Chem Res 2009;42:925-937.
10. Bozoklu GI, Gateau C, Imbert D, Pécaut J, Robeyns K, Filinchuk Y, Memon F, Muller G, Mazzanti M. Metal-Controlled Diastereoselective Self-Assembly and Circularly Polarized Luminescence of a Chiral Heptanuclear Europium Wheel. J Am Chem Soc 2012;134:8372-8375.
11. Huang C-H. Rare earth coordination chemistry: Fundamentals and applications: John Wiley & Sons; 2010.
12. Bünzli J-CG, Comby S, Chauvin A-S, Vandevyver CDB. New Opportunities for Lanthanide Luminescence. J Rare Earth 2007;25:257-274.
13. Vuojola J, Soukka T. Luminescent lanthanide reporters: new concepts for use in bioanalytical applications. Methods Appl Fluoresc 2014;2:012001.
14. McGehee MD, Bergstedt T, Zhang C, Saab AP, O'Regan MB, Bazan GC, Srdanov VI, Heeger AJ. Narrow bandwidth luminescence from blends with energy transfer from semiconducting conjugated polymers to europium complexes. Adv Mater (Weinheim, Ger) 1999;11:1349-1354.
15. Evans RC, Douglas P, Winscom CJ. Coordination complexes exhibiting room-temperature phosphorescence: evaluation of their suitability as triplet emitters in organic light emitting diodes. Coord Chem Rev 2006;250:2093-2126.
16. Giovanella U, Pasini M, Freund C, Botta C, Porzio W, Destri S. Highly efficient color-tunable OLED based on poly (9, 9-dioctylfluorene) doped with a novel europium complex. J Phys Chem C 2009;113:2290-2295.
17. Klampaftis E, Ross D, McIntosh KR, Richards BS. Enhancing the performance of solar cells via luminescent down-shifting of the incident spectrum: a review. Sol Energy Mater Sol Cells 2009;93:1182-1194.
18. Bünzli J-CG, Eliseeva SV. Lanthanide NIR luminescence for telecommunications, bioanalyses and solar energy conversion. J Rare Earth 2010;28:824-842.
19. Muller G. Luminescent chiral lanthanide (III) complexes as potential molecular probes. Dalton Trans 2009:9692-9707.
20. Lunkley JL, Shirotani D, Yamanari K, Kaizaki S, Muller G. Extraordinary circularly polarized luminescence activity exhibited by cesium tetrakis (3-heptafluoro-butylryl-(+)-camphorato) Eu (III) complexes in EtOH and CHCl3 Solutions. J Am Chem Soc 2008;130:13814-13815.
21. Circularly polarized luminexence: A probe for chirality in the excited state. In: N. Berova, K. Nakanishi, Woody RW, editors. Circular Dichroism: Principles and Applications. New York: Wiley-VCH; H. P. J. M. Dekkers. p 185-215.
22. Richardson FS. Selection rules for lanthanide optical activity. Inorg Chem 1980;19:2806-2812.
23. Petoud S, Muller G, Moore EG, Xu J, Sokolnicki J, Riehl JP, Le UN, Cohen SM, Raymond KN. Brilliant Sm, Eu, Tb,

and Dy chiral lanthanide complexes with strong circularly polarized luminescence. J Am Chem Soc 2007;129:77-83.
24. Lunkley JL, Shirotani D, Yamanari K, Kaizaki S, Muller G. Chiroptical Spectra of a Series of Tetrakis ((+)-3-heptafluorobutylyrylcamphorato) lanthanide (III) with an Encapsulated Alkali Metal Ion: Circularly Polarized Luminescence and Absolute Chiral Structures for the Eu (III) and Sm (III) Complexes. Inorg Chem 2011;50:12724-12732.
25. Seitz M, Moore EG, Ingram AJ, Muller G, Raymond KN. Enantiopure, octadentate ligands as sensitizers for europium and terbium circularly polarized luminescence in aqueous solution. J Am Chem Soc 2007;129:15468-15470.
26. Bauer H, Blanc J, Ross DL. Octacoordinate chelates of lanthanides. Two series of compounds. J Am Chem Soc 1964;86:5125-5131.
27. Samuel AP, Lunkley JL, Muller G, Raymond KN. Strong Circularly Polarized Luminescence from Highly Emissive Terbium Complexes in Aqueous Solution. Eur J Inorg Chem 2010;2010:3343-3347.
28. Dickins RS, Parker D, Bruce JI, Tozer DJ. Correlation of optical and NMR spectral information with coordination variation for axially symmetric macrocyclic Eu (III) and Yb (III) complexes: axial donor polarisability determines ligand field and cation donor preference. Dalton Trans 2003:1264-1271.
29. Riehl JP, Muller G. Circularly Polarized Luminescence Spectroscopy and Emission-Detected Circular Dichroism. In: Berova N, Polavarapu PL, Nakanishi K, Woody RW, editors. Comprehensive Chiroptical Spectroscopy. Volume 1: Wiley; 2012.
30. Brittain HG, Desreux JF. Luminescence and NMR studies of the conformational isomers of lanthanide complexes with an optically active polyaza polycarboxylic macrocycle. Inorg Chem 1984;23:4459-4466.
31. Aime S, Botta M, Fasano M, Marques MPM, Geraldes CF, Pubanz D, Merbach AE. Conformational and coordination equilibria on DOTA complexes of lanthanide metal ions in aqueous solution studied by 1H-NMR spectroscopy. Inorg Chem 1997;36:2059-2068.
32. Di Bari L, Pintacuda G, Salvadori P. Stereochemistry and near-infrared circular dichroism of a chiral Yb complex. J Am Chem Soc 2000;122:5557-5562.
33. Di Bari L, Salvadori P. Static and Dynamic Stereochemistry of Chiral Ln DOTA Analogues. ChemPhysChem 2011;12:1490-1497.
34. Haas Y, Stein G. Quenching of the fluorescence of rare earth ions by high energy vibrations of solvent molecules: calculations of Franck-Condon factors from spectral data. Chem Phys Lett 1972;15:12-16.
35. Stein G, Würzberg E. Energy gap law in the solvent isotope effect on radiationless transitions of rare earth ions. J Chem Phys 2008;62:208-213.
36. Law G-L, Andolina CM, Xu J, Luu V, Rutkowski PX, Muller G, Shuh DK, Gibson JK, Raymond KN. Circularly Polarized Luminescence of Curium: A New Characterization of the 5f Actinide Complexes. J Am Chem Soc 2012;134:15545-15549.
37. Seitz M, Do K, Ingram AJ, Moore EG, Muller G, Raymond KN. Circularly Polarized Luminescence in Enantiopure Europium and Terbium Complexes with Modular, All-Oxygen Donor Ligands. Inorg Chem 2009;48:8469-8479.
38. Beeby A, M. Clarkson I, S. Dickins R, Faulkner S, Parker D, Royle L, S. de Sousa A, A. Gareth Williams J, Woods M. Non-radiative deactivation of the excited states of europium, terbium and ytterbium complexes by proximate energy-matched OH, NH and CH oscillators: an improved luminescence method for establishing solution hydration states. J Chem Soc Perk T 2 1999:493-504.
39. Malta O, Brito H, Menezes J, Gonçalves e Silva F, de Mello Donegá C, Alves Jr S. Experimental and theoretical emission quantum yield in the compound Eu (thenoyltrifluoroacetonate)3• 2 (dibenzyl sulfoxide). Chem Phys Lett 1998;282:233-238.
40. Freund C, Porzio W, Giovanella U, Vignali F, Pasini M, Destri S, Mech A, Di Pietro S, Di Bari L, Mineo P. Thiophene based europium β-diketonate complexes: effect of the ligand structure on the emission quantum yield. Inorg Chem 2011;50:5417-5429.
41. Schippers P, van den Buekel A, Dekkers H. An accurate digital instrument for the measurement of circular polarisation of luminescence. J Phys E 1982;15:945.
42. Riehl JP, Richardson FS. Circularly polarized luminescence spectroscopy. Chem Rev 1986;86:1-16.
43. Bonsall SD, Houcheime M, Straus DA, Muller G. Optical isomers of N, N′-bis (1-phenylethyl)-2, 6-pyridinedicarboxamide coordinated to europium (III) ions as reliable circularly polarized luminescence calibration standards. Chem Commun 2007:3676-3678.
44. Harada T, Nakano Y, Fujiki M, Naito M, Kawai T, Hasegawa Y. Circularly polarized luminescence of Eu (III) complexes with point-and axis-chiral ligands dependent on coordination structures. Inorg Chem 2009;48:11242-11250.
45. Harada T, Tsumatori H, Nishiyama K, Yuasa J, Hasegawa Y, Kawai T. Nona-Coordinated Chiral Eu (III) Complexes with Stereoselective Ligand–Ligand Noncovalent Interactions for Enhanced Circularly Polarized Luminescence. Inorg Chem 2012;51:6476-6485.
46. Yuasa J, Ohno T, Miyata K, Tsumatori H, Hasegawa Y, Kawai T. Noncovalent Ligand-to-Ligand Interactions Alter Sense of Optical Chirality in Luminescent Tris (β-diketonate) Lanthanide (III) Complexes Containing a Chiral Bis (oxazolinyl) Pyridine Ligand. J Am Chem Soc 2011;133:9892-9902.
47. Tsumatori H, Harada T, Yuasa J, Hasegawa Y, Kawai T. Circularly Polarized Light from Chiral Lanthanide(III) Complexes in Single Crystals. Appl Phys Express 2011;4:011601.
48. Mamula O, Lama M, Telfer SG, Nakamura A, Kuroda R, Stoeckli‐Evans H, Scopelitti R. A Trinuclear EuIII Array within a Diastereoselectively Self‐Assembled Helix Formed by Chiral Bipyridine‐Carboxylate Ligands. Angew Chem 2005;117:2583-2587.
49. Evans NH, Carr R, Delbianco M, Pal R, Yufit DS, Parker D. Complete stereocontrol in the synthesis of macrocyclic lanthanide complexes: direct formation of enantiopure systems for circularly polarised luminescence applications. Dalton Trans 2013;42:15610-15616.
50. Carr R, Evans NH, Parker D. Lanthanide complexes as chiral probes exploiting circularly polarized luminescence. Chem Soc Rev 2012;41:7673-7686.
51. Butler SJ, Lamarque L, Pal R, Parker D. EuroTracker dyes: highly emissive europium complexes as alternative organelle stains for live cell imaging. Chemical Science 2014;5:1750-1756.
52. Metcalf DH, Snyder SW, Wu S, Hilmes GL, Riehl JP, Demas JN, Richardson FS. Excited-state chiral discrimination observed by time-resolved circularly polarized luminescence measurements. J Am Chem Soc 1989;111:3082-3083.
53. Das Gupta A, Richardson FS. Spectroscopic studies of lanthanide ion binding to multidentate ligands in aqueous solution. 3. Optically active Tb(EHPG)(L)n and Tb(DPA)m(L)n complexes. Inorg Chem 1981;20:2616-2622.
54. Moussa A, Pham C, Bommireddy S, Muller G. Importance of hydrogen‐bonding sites in the chiral recognition mechanism between racemic D3 terbium (III) complexes and amino acids. Chirality 2009;21:497-506.
55. Kirschner S, Bakkar I. Utilization of the pfeiffer effect and outer-sphere complexation for the prediction of absolute configurations of optically active metal complexes. Coord Chem Rev 1982;43:325-335.
56. Pescitelli G, Di Bari L, Berova N. Application of electronic circular dichroism in the study of supramolecular systems. Chem Soc Rev 2014.
57. Carr R, Di Bari L, Lo Piano S, Parker D, Peacock RD, Sanderson JM. A chiral probe for the acute phase proteins alpha-1-acid glycoprotein and alpha-1-antitrypsin based on europium luminescence. Dalton Trans 2012;41:13154-13158.
58. Montgomery CP, New EJ, Parker D, Peacock RD. Enantioselective regulation of a metal complex in

reversible binding to serum albumin: dynamic helicity inversion signalled by circularly polarised luminescence. Chem Commun 2008:4261-4263.
59. Dias DM, Teixeira JMC, Kuprov I, New EJ, Parker D, Geraldes CFGC. Enantioselective binding of a lanthanide(iii) complex to human serum albumin studied by 1H STD NMR techniques. Org Biomol Chem 2011;9:5047-5050.
60. Smith DG, McMahon BK, Pal R, Parker D. Live cell imaging of lysosomal pH changes with pH responsive ratiometric lanthanide probes. Chem. Commun. 2012;48:8520-8522.
61. Richardson FS, Faulkner TR. Optical activity of the f–f transitions in trigonal dihedral (D3) lanthanide (III) complexes. I. Theory. J Chem Phys 1982;76:1595-1606.
62. Di Bari L, Salvadori P. Solution structure of chiral lanthanide complexes. Coord Chem Rev 2005;249:2854-2879.
63. Di Pietro S, Piano SL, Di Bari L. Pseudocontact shifts in lanthanide complexes with variable crystal field parameters. Coord Chem Rev 2011;255:2810-2820.
64. Bruce JI, Parker D, Lopinski S, Peacock RD. Survey of factors determining the circularly polarised luminescence of macrocyclic lanthanide complexes in solution. Chirality 2002;14:562-567.
65. Di Pietro S, Di Bari L. The Structure of MLn (hfbc) 4 and a Key to High Circularly Polarized Luminescence. Inorg Chem 2012;51:12007-12014.
66. Mason S. Molecular optical activity and the chiral discriminations.: Cambridge University Press; 1982.
67. Di Pietro S. Synthesis, structural and dynamic investigation of chiral metal complexes. [PhD thesis]: University of Pisa; 2012.
68. Castiglioni E, Abbate S, Longhi G. Revisiting with updated hardware an old spectroscopic technique: circularly polarized luminescence. Appl Spectrosc 2010;64:1416-1419.
69. Emeis C, Oosterhoff L. Emission of circularly-polarised radiation by optically-active compounds. Chem Phys Lett 1967;1:129-132.
70. Dekkers HP, Emeis C, Oosterhoff LJ. Measurement of optical activity in racemic mixtures. J Am Chem Soc 1969;91:4589-4590.
71. Emeis CA, Oosterhoff LJ. The n - π* Absorption and Emission of Optically Active trans - β - Hydrindanone and trans - β - Thiohydrindanone. J Chem Phys 1971;54:4809-4819.
72. Herren M, Morita M. Near-infrared circular polarized luminescence spectroscopy of GMO: Er3+ crystals. J Lumin 1995;66:268-271.
73. Maupin CL, Parker D, Williams JG, Riehl JP. Circularly polarized luminescence from chiral octadentate complexes of Yb (III) in the near-infrared. J Am Chem Soc 1998;120:10563-10564.
74. Maupin CL, Dickins RS, Govenlock LG, Mathieu CE, Parker D, Williams JG, Riehl JP. The measurement of circular polarization in the near-IR luminescence from chiral complexes of Yb (III) and Nd (III). J Phys Chem A 2000;104:6709-6717.